Electronic Supplementary Material (ESI) for Dalton Transactions.

Supporting information

A-site cation with high vibrational motion in ABX_3 perovskite effectively induce dielectric phase transition

Yu-zhen Wang,[ab] Zhi-Xu Zhang,[a] Chang-Yuan Su,[a] Tie Zhang,[a] Da-Wei Fu*[ab] and Yi Zhang*[a]

(a Ordered Matter Science Research Center, Jiangsu Key Laboratory for Science and Applications of Molecular Ferroelectrics, Southeast University, Nanjing, 211189, People's Republic of China.

b Institute for Science and Applications of Molecular Ferroelectrics, Key Laboratory of the Ministry of Education for Advanced Catalysis Materials, Zhejiang Normal University, Jinhua, 321004, People's Republic of China.)

Experimental Measurement Methods

Variable temperature X-ray crystallography

The crystal diffraction data of [FMPD][$Cd(SCN)_3$] were collected on Rigaku Saturn 724 diffractometer with Mo Kα diffraction (λ = 0.7107 3 Å) at 273 K and 333 K. And the data processing including empirical absorption correction was carried out with crystal clear software package. The crystal structures of [FMPD][$Cd(SCN)_3$] before and after phase transition were solved by direct method and refined by the full matrix least-squares method based on F^2 in the SHELXTL program package. All the H atoms are geometrically generated at the appropriate positions, while the other atoms are refined by all reflections of $I > 2\sigma$ (I). The minimum asymmetric unit and packing view of the crystal structure were drawn by DIAMOND software. Other specific crystallographic data and structure refinements details are given in Table S1.

Other measurements

The heating and cooling cycle measurements of the dielectric constant and the dielectric loss were performed on the Tonghui TH2828A instrument at frequencies of 5 kHz, 10 kHz, 100 kHz, and 1 MHz respectively. The compressed tablet and single crystal samples of [FMPD][$Cd(SCN)_3$] deposited with silver conductive glue were used as the electrode in the dielectric measurement. The differential scanning calorimetry (DSC) measurement was performed on the PerkinElmer diamond DSC instrument under a nitrogen atmosphere. The powder sample of [FMPD][Cd(SCN)$_3$] (10.3 mg) experienced heating and cooling cycle measurement in the temperature range of 240 K to 375 K at a scan rate of 20 K min^{-1}. IR spectra were conducted on a Shimadzu IR Prestige-21. Variable-temperature powder X-ray diffraction (PXRD) measurements were performed on a Rigaku D/MAX 2000 PC X-ray diffractometer. The PXRD patterns were collected in the 2θ range of 5°-50° with a step size of 0.02°. Thermogravimetric analysis (TGA) was performed on a TA Q50 system at a heating rate of 10 K min^{-1} in the nitrogen atmosphere.

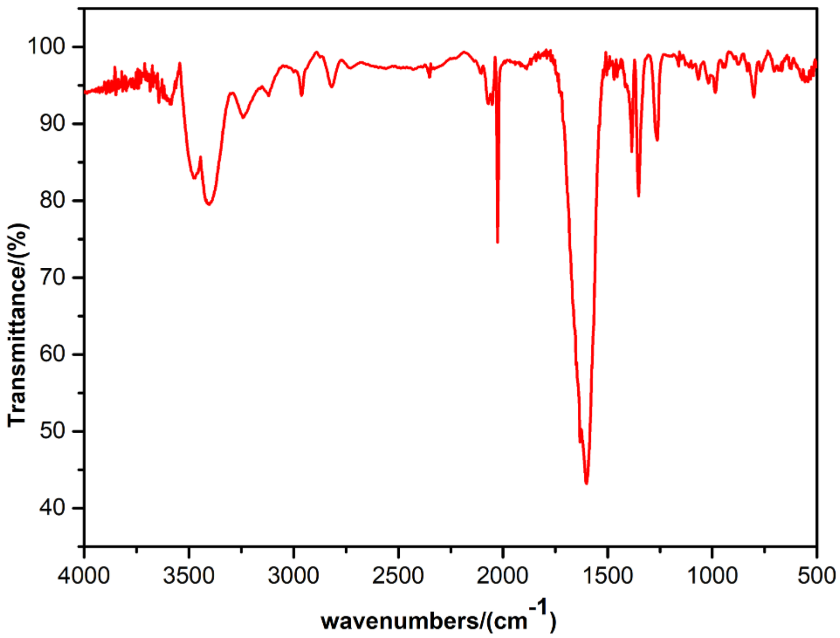

Fig S1. Infrared spectrum of [FMPD][Cd(SCN)$_3$].

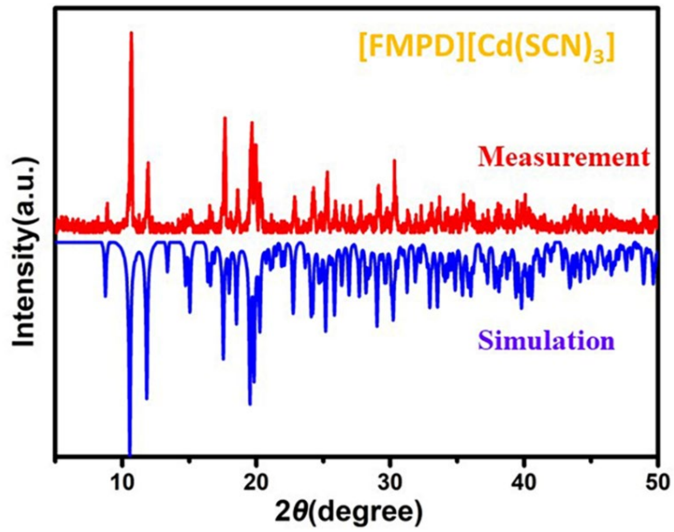

Fig S2. Comparison between measurement and simulation PXRD of [FMPD][Cd(SCN)$_3$].

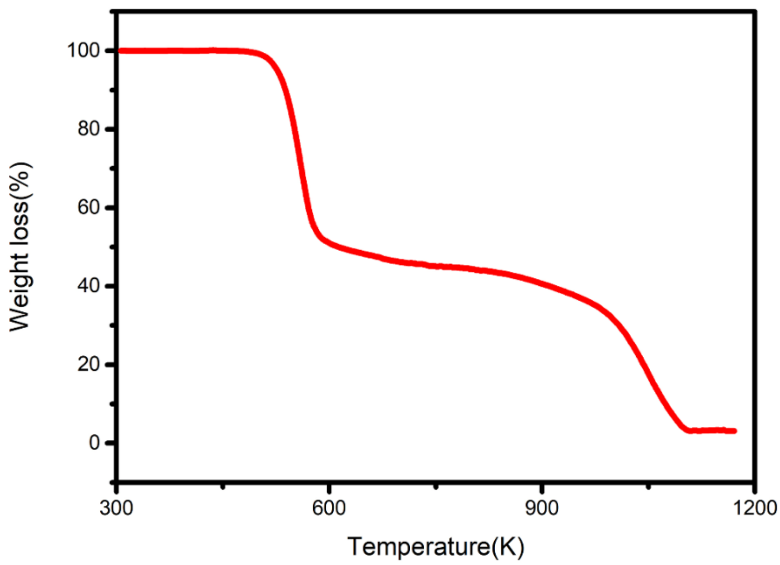

Fig S3. TGA curve of [FMPD][Cd(SCN)$_3$].

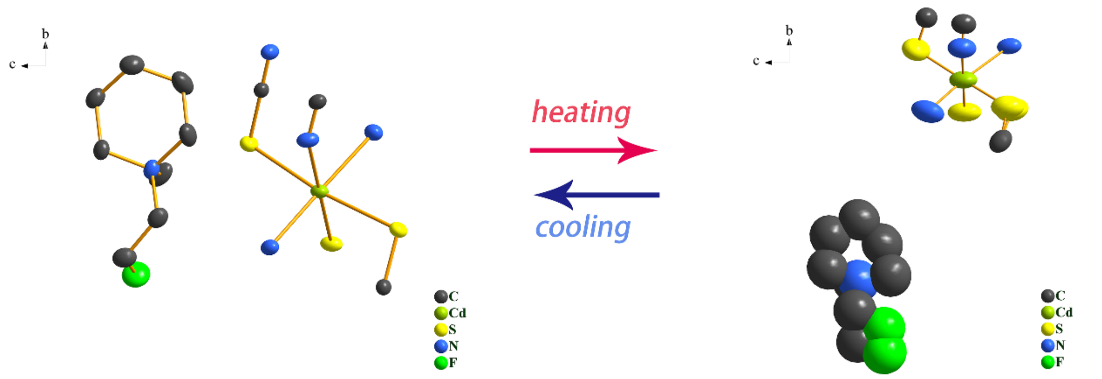

Fig S4. LTP and ITP thermal ellipsoid probability diagram of the smallest asymmetric unit.

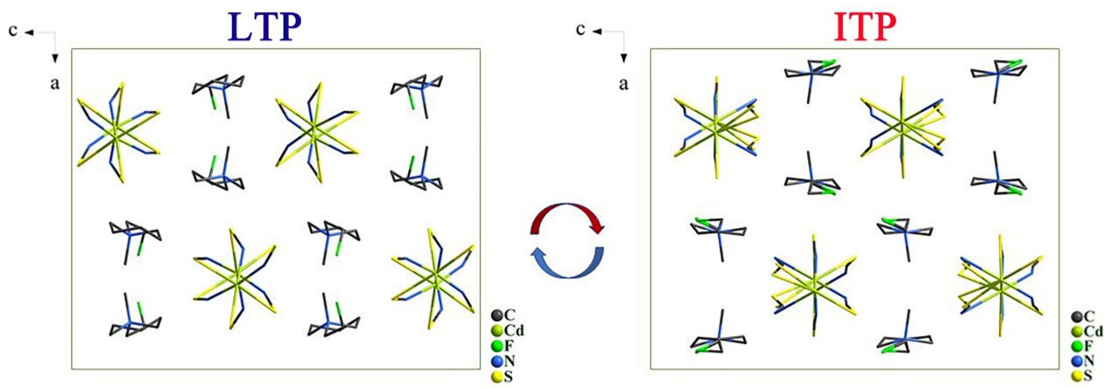

Fig S5. Packing of [FMPD][Cd(SCN)$_3$] in LTP and ITP from the perspective of b-axis.

Table S1. Crystal data and structure refinements for [FMPD][Cd(SCN)$_3$] at 273 K and 333 K.

	LTP (273K)	**ITP (333K)**
Empirical formula	$C_{11}H_{17}N_4CdFS_3$	$C_{11}H_{17}N_4CdFS_3$
Formula weight	432.88	432.88
Crystal system	orthorhombic	orthorhombic
Space group	*Pbca*	*Pbca*
a/ **Å**	14.9579(13)	16.4557(13)
b/ **Å**	10.8069(7)	10.7894(5)
c/ **Å**	20.2117	19.3242(19)
α/ **°**	90	90
β/ **°**	90	90
γ/ **°**	90	90
Volume/ **Å^3**	3267.19(50)	3430.96(50)
Z	8	8
F (000)	1728.0	1592.0
GOF	1.074	1.658
R_1[I > 2σ(I)]	0.0323	0.1822
wR_2[I > 2σ(I)]	0.0559	0.4447

Table S2. Selected bond lengths and bond angles for [FMPD][Cd(SCN)$_3$] at 273 K and 333 K.

Temperature	Bond lengths [Å]		Bond angles [°]	
273 K	C1—C2	1.514(2)	C3—C2—C1	111.77(16)
	C5—N1	1.520(2)	C2—C3—C4	110.56(18)
	C7—N1	1.517(2)	C3—C4—C5	110.55(19)
	C8—F1	1.382(3)	C4—C5—N1	113.26(16)
	C9—N2	1.1480(19)	C8—C7—N1	116.96(15)
	C9—S3	1.6435(15)	F1—C8—C7	111.15(19)
	C10—N4	1.156(2)	N2—C9—S3	178.64(15)
	C10—S1	1.6413(16)	N2—Cd1—N4	89.69(5)
	C11—N3	1.1589(19)	N2—Cd1—S1	93.76(4)
	C11—S2	1.6387(15)	N2—Cd1—S3	96.70(4)
	Cd1—N2	2.2932(14)	C6—N1—C1	110.37(14)
	Cd1—N4	2.3353(15)	C6—N1—C7	109.62(15)
	Cd1—S1	2.6888(5)	C1—N1—C7	110.41(13)
	Cd1—S2	C2.7671(5)	C6—N1—C5	110.74(17)
	N2—C9	1.1479(19)	C1—N1—C5	108.73(14)
	N3—Cd1	2.3407(14)	C7—N1—C5	106.91(13)
	S1—C10	1.6412(16)	C9—N2—Cd1	152.91(13)
			C10—N4—Cd1	142.13(14)
333 K	C1—C2	1.5001(14)	C3—C2—C1	120.91(15)
	C5—N1	1.5001(12)	C4—C3—C2	103.68(11)
	C7—N1	1.5002(12)	C3—C4—C5	144.7(2)
	C8A—F1A	1.3802(16)	N1—C5—C4	80.42(8)
	C9—N2	1.265(5)	C8B—C7—N1	129.08(13)
	C9—S3A	1.568(5)	C8A—C7—N1	130.75(14)
	C10—N4	1.156(5)	F1A—C8A—C7	105.9(2)
	C10—S1	1.610(4)	N2—C9—S3A	165.5(5)
	C11—N3	1.280(3)	N2—C9—S3B	165.1(5)
	C11—S2B	1.5668(19)	N4—Cd1—N2	92.68(15)
	Cd1—N2	2.316(5)	N2—Cd1—S1	91.87(11)
	Cd1—N4	2.289(5)	N2—Cd1—S3B	87.21(15)
	Cd1—S1	2.7289(17)	C6—N1—C1	92.4(3)

Cd1—S2	2.7671(5)	C6—N1—C7	111.1(4)
N2—C9	1.265(5)	C1—N1—C7	98.20(19)
S1—C10	1.610(4)	C5—N1—C7	97.25(19)
		C9—N2—Cd1	136.9(4)
		C10—N4—Cd1	149.3(4)